5-2012

SYNthesis, CHARACTERIZATION AND APPLICATIONS OF DIFFERENT NANOSTRUCTURES

Whitney Snyder
Clemson University, wsnyder@g.clemson.edu

SYNTHESIS, CHARACTERIZATION AND APPLICATIONS OF DIFFERENT NANOSTRUCTURES

A Thesis
Presented to
the Graduate School of
Clemson University

In Partial Fulfillment
of the Requirements for the Degree
Master of Science
Chemistry

---

by
Whitney Elaine Snyder
August 2012

Accepted by:
Dr. George Chumanov, Committee Chair
Dr. Kenneth Christensen
Dr. Jeffery Anker
Dr. Gautum Bhattacharyya

ABSTRACT

There has been a growing interest in the field of nanoscience for the last several decades including the use in optical, electrical, biological and medicinal applications. This thesis focuses on the synthesis of different nanoparticles for their potential uses in drug delivery and antimicrobial agents as well as porous alumina membranes as surface enhanced Raman scattering or SERS substrates.

The synthesis of nanocomposites (NCs) composed of silica and poly(4-vinyl pyridine) (P4VP) in a basic ethanol solution is presented in chapter 2. The composition of the NCs appears to be homogenous after synthesis and is greatly affected by heat and pH changes. When the NCs are heated, a core-shell nanostructure is produced with silica forming a shell around a P4VP core. At lower pHs, the NCs form a silica core with a P4VP shell while at higher pHs the silica is etched away causing the NC to decompose.

A novel synthesis method of growing stable copper oxide nanoparticles with poly(acrylic acid) (PAA) is presented in chapter 3. Insoluble copper (I) oxide is dissolved with ammonium hydroxide and reduced using sodium borohydride to form metallic copper nanoparticles that oxidize overtime to form copper oxide nanoparticles stable in an aqueous environment. In addition to copper oxide nanoparticles, copper (I) iodide and copper (II) sulfide particles were also synthesized in the presence of PAA.

In chapter 4, alumina membranes with 100nm and 200nm pores were coated with silver and used as SERS substrates to detect small molecules. The alumina membranes are coated with silver by reducing silver (I) oxide with ethanol. The thickness of the silver layer depends primarily on the length of time the substrate comes into contact with

the Ag_2O in solution with longer exposure times producing thicker films. Raman scattering of 10-100nM adenine concentrations were collected.

DEDICATION

I dedicate this thesis to my mom, Linda Snyder for her constant love and support throughout my life. I also dedicate this to all my friends and family who without them I would not be where I am today.

ACKNOWLEDGMENTS

First I would like to acknowledge my advisor, Dr. George Chumanov for his guidance and encouragement throughout my graduate school experience. I would also like to acknowledge all my past and present group members: John Heckel, Kyle Dukes, Zachary Koontz, Aubrie Pfirman, Joseph Mannion, Daniel Willett, Brad Durbin and Russell Cooper for all their support and helpful discussions. I would like to thank the Clemson University Department of Chemistry, especially my committee members for giving me this opportunity to grow as a chemist.

TABLE OF CONTENTS

Table of Contents (Continued)

Page

LIST OF TABLES

Table Page

LIST OF FIGURES

CHAPTER ONE

INTRODUCTION

There has been a growing interest in the study and synthesis of nanoparticles (NPs) over the last several decades. Their potential use in biological,[1] medical,[1] electronic,[2] and optical[2] applications are some of the driving forces for their synthesis. A few examples of NPs used for biological systems or in medicine include fluorescent labels[1,3] and drug delivery and therapeutics.[4,5,6] For NP uses in drug delivery the surface needs to have a coating, such as antibodies that will allow it to interact with cells. Core-shell nanostructures are one potential way to get a coating on the outside of a NP. There are many core-shell possibilities including metal-metal,[7,8] metal-dielectric,[9,10,11] and polymer-dielectric.[12] For drug delivery the most popular core-shell nanostructure are polymer-polymer[13] and mesoporous silica nanoparticles coated with polymers.[14]

Here, the synthesis of nanocomposites composed of silica and poly(4-vinyl pyridine) (P4VP) which have the potential to be used in drug delivery is discussed. The synthesis is based on a procedure reported by Serchtook and Avnir[15] where large nanocomposites composed of silica and polystyrene (PS) were synthesized. When using PS, a surfactant is needed, so P4VP was used in its place. When heated the silica/P4VP nanocomposites have been shown to form a core-shell nanostructure which can be explored for its use in drug delivery applications. In addition to heat, pH also affects the structure of the nanocomposites and at lower pHs they will form core-shell nanostructures. If the shells of the nanostructures are silica, the surfaces can easily be

modified with molecules to aid in cell uptake. Different polymers may also be used to aid in cell interactions.

Not only can silica/polymer nanostructures be used in biological systems, noble metal NPs also have this potential. Both silver and copper have been found to have antimicrobial properties which are of great interest due to their use as disinfectants in health care as well as in wastewater treatments.[16,17] However they are both considered cytotoxic which limits their use, especially in biological systems. Like the previously discussed core-shell nanostructures, the surface of the metal NPs will need to be modified first which is often done in the synthesis process. Noble metal NPs typically will aggregate in solution unless a surfactant or other capping agent is added to keep them suspended. The capping agent can serve a dual purpose of keeping the NP suspended and allowing them to be stable around biological samples.

Here, a new method of forming copper oxide nanoparticles in the presence of poly(acrylic acid) (PAA) used as a stabilizing agent is presented. Most methods for growing copper nanoparticles with poly(acrylic acid) (PAA) as a stabilizing agent uses soluble copper salts, such as copper (II) sulfate[18,19,20] and copper (II) acetate,[21] however we developed a method that uses copper (I) oxide dissolved ammonium hydroxide. Copper (II) sulfide and copper (I) iodide particles were also synthesized in the presence of PAA using simple double displacement reactions with aqueous copper (II) sulfate. Modification can take place on either the copper surface or on the PAA chains depending on how the two entities interact. Once the copper particles are modified, they can be used as disinfectants in various medical and health care situations.

In addition to having antimicrobial properties both copper and silver exhibit unique optical properties due to the excitation of plasmon resonances, which are the collective oscillation of the conduction electrons. Although copper does show plasmon resonances, it does not interact nearly as strong as silver does with light. Due to silver's strong interaction with light, it has been widely explored as a SERS substrate. SERS was first discovered in the mid-70's by Fleischmann et al.[22] and Jeanmarie and Van Duyne[23] after noticing an increase Raman signal from molecules adsorbed onto the surface of roughened electrodes. In normal Raman spectroscopy there is a small scattering cross-section for molecules which presents a disadvantage. However, when using a SERS substrate, the signal can be enhanced up to 10^{10}.[24] In SERS, Raman scattering organic molecules are either adsorbed onto or in close proximity of the surface of the substrate (i.e. silver). When the incident light excites the localized plasmon resonances of the substrate an enhanced Raman scattering signal from the organic molecule is detected. This strong enhancement is due to the increased local electric fields at the surface of the metal and when the surface is imperfect or not smooth, then hot spots or junctions are formed.[25] The hot spots are areas of strong electromagnetic coupling from the different parts of the sample.[26,27] If two nanoparticles are in close proximity, then their individual electric fields interact making the hot spot in between the particles, phenomenon known as plasmon coupling.

The first SERS active substrates used were roughened electrodes.[22,23] Since then, many different types of roughened substrates have been used such as island films[28] and colloids.[29] Different types of alumina with silver deposited on the surfaces have been

used as substrates including alumina particles[30,31] tunable arrays[32] and membranes.[33] The silver is typically deposited in one of three ways, either by chemically or vapor depositing silver onto the surface of the alumina as well as filtering colloids through the pores. Here, porous alumina membranes are used as SERS substrates after coating with silver by a simple ethanol reduction. The benefit of using a porous membrane is that dilute organic solutions can be filtered through the pores concentrating the sample which in addition to the increased enhancement due to SERS a stronger Raman signals. Dilute adenine solutions (10-100nM) were filtered through the silver coated alumina membranes and were shown to produce a strong Raman signal.

In the following manuscript the three different nanostructures mentioned above are discussed in more detail. Chapter 2 will focus on the synthesis of the nanocomposites composed of silica and P4VP. The effects of pH and heat on the structure of the nanocomposites are also reported in chapter 2. The synthesis of different copper particles in the presence of PAA are reported in chapter 3. In chapter 4, the use of porous alumina membranes as SERS substrates is discussed. The membranes were coated by the reduction of Ag_2O by ethanol and adenine was used to monitor SERS activity.

CHAPTER TWO

SYNTHESIS OF NANOCOMPOSITES COMPOSED OF SILICA AND POLY(4-VINYLPYRIDINE)

Introduction

Nanocomposites were first synthesized for their potential use in core/shell nanostructures where the core would be composed of a dielectric medium, such as silica, and the shells would be silver. Due to the difficulty of growing a continuous silver shell around a silica nanoparticle, it was thought by adding a polymer to the silica synthesis the chances of the silver attaching to the surface would increase. The syntheses of the NCs presented here are based on the procedure written by Sertchook and Avnir[15] which developed silica/polystyrene nanocomposites. Since polystyrene is insoluble in ethanol, a surfactant was needed in order to keep the styrene suspended in the solution while the silica was being hydrolyzed. We modified the procedure by replacing the polystyrene with poly(4-vinyl pyridine) (P4VP) which has a higher affinity for silver than polystyrene. Another benefit of using P4VP is that it is soluble in ethanol which will eliminate the need for a surfactant in the synthesis. The benefit of using P4VP is that not only does pyridine have a high affinity for silver, but it is also soluble in ethanol which eliminates the need for a surfactant. As mentioned in the introduction, NCs have many potential applications including their use in core/shell nanostructures and drug delivery.

Experimental Methods

Materials: 160,000 MW Poly(4-vinyl pyridine) (P4VP) was purchased from Sigma Aldrich. 98% Tetraethoxysilane (TEOS) was purchased from Alfa Aesar. 29.3%

ammonium hydroxide was purchased from Fisher Scientific. Absolute 200 proof ethanol was received from Pharmco-AAPER.

Nanocomposites Synthesis: In a typical procedure, a 1% w/w P4VP solution in ethanol was used in all NC synthesis. In a 20mL scintillation vial, 10mL of absolute ethanol and 800µL 29% NH_4OH was stirred vigorously. In a 1dr vial, 1mL ethanol, TEOS (250-600µL) and P4VP (250-600µL) was briefly sonicated before dumping the contents into the ethanol/NH_4OH solution and allowing them to roll overnight. After aging overnight the nanocomposites were washed three times with ethanol by centrifugation and in some experiments the solvents were switched to water in the same manner.

Segregation Method: In a typical heating procedure, 1mL of cleaned NCs (in water or ethanol) was added to 100mL of 18MΩ water in a round bottom flask. The NCs were heated at 70°C for 4 hours while stirring.

Characterization: The NCs were dried on a formvar coated copper grid purchased from Ted Pella and imaged using the TEM-Hitachi H7600T.

Results and Discussion

The synthesis of the NCs is based on the well-known Stöber synthesis method.[34] The reaction for plain silica nanoparticles using TEOS and ammonium hydroxide as a catalyst is as follows[35,36]:

$$Si(OC_2H_5)_4 + xH_2O \leftrightarrow [Si(OC_2H_5)_{4-x}(OH)_x] + xC_2H_5OH \leftrightarrow Si(OH)_4 + 4C_2H_5OH \quad (1)$$

$$2Si(OH)_4 \rightarrow 2\,(Si\text{-}O\text{-}Si) + 4H_2O \quad (2)$$

P4VP is added in the first step of reaction (1) in order to incorporate the polymer throughout the NC. The size of the NCs is easily controlled by adjusting the amounts of TEOS, ammonium hydroxide and P4VP added and can be summarized in Table 2.1. Higher concentrations of ammonium hydroxide produced larger nanoparticles which is typical of silica nanoparticle synthesis. Initially you form more of the intermediate $[Si(OC_2H_5)_{4-x}(OH)_x]$ quickly in order to produce more seeds which in turn aggregate into larger particles during the condensation reaction (2). As the concentration of P4VP is increased, the size decreases which is seen when comparing NC14 and NC16 in Table 2.1. An explanation for this occurrence is that as the number of polymer chains increases, the number of seeds available also increases for the silica to hydrolyze around which decreases the size of the nanoparticles but allows for more to be formed.

Table 2.1. Concentration of starting material in silica/poly(4-vinyl pyridine) nanocomposites and the corresponding sizes.

Sample	TEOS (M)	P4VP (M) ($x10^{-4}$)	NH_4OH (M)	Size (nm)
3	0.19	2.5	1.3	35.4 ± 5.5
8	0.15	2.4	2.1	261 ± 9
14	0.15	2.4	1.7	118.2 ± 24.8
16	0.15	3.9	1.7	83.5 ± 6.7

After the initial experiments to determine the optimum concentrations for the sizes desired, the typical concentrations of the TEOS was 0.15M and the ammonium hydroxide was kept at 1.7M for the procedures. Only the P4VP concentrations were

adjusted to determine what size NC was produced. The initial goal of the project was to grow a silver shell around the core of the NC. The first method used to try to grow a silver shell was based on the procedure done by Evanoff et. al.[37] This method produced an interesting result where the NCs became segregated internally. NCs that were stored in an ethanol solution were placed in a reaction vessel with Ag_2O and water. The vessel

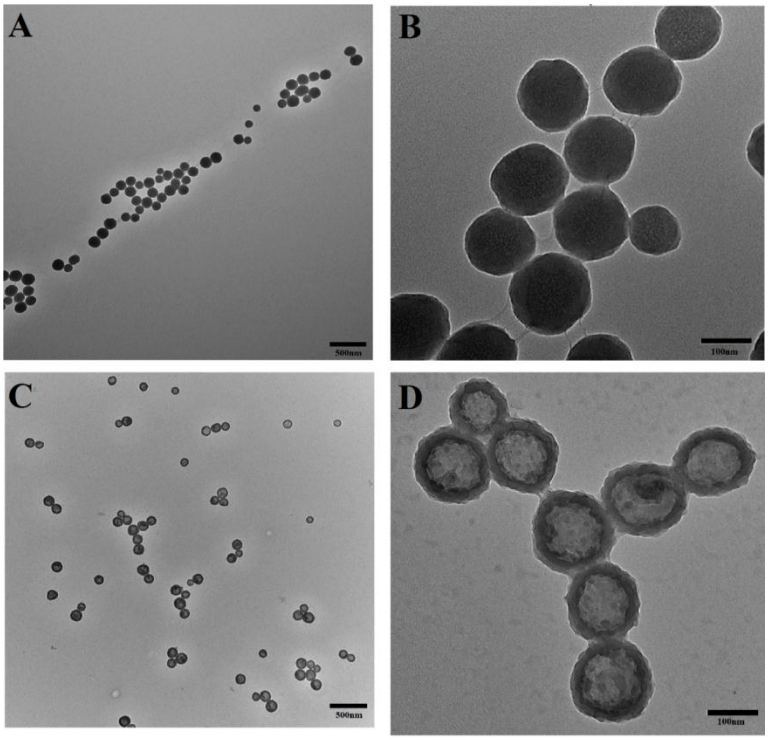

Figure 2.1. TEM images of silica/poly(4-vinyl pyridine) nanocomposites before heating (A,B) and after heating at 70°C for 4hrs (C,D).

was heated to 70°C and pressurized at 10psi for approximately 4 hours. It was noticed that the Ag_2O was reduced to silver nanoparticles in the solution but did not reduce onto the surface of the NCs. The NCs, however became segregated and formed a core-shell nanostructure. The reaction was repeated without the prescence of Ag_2O, and again the

NCs became segregated. Figure 2.1 shows the NCs before being heated (A,B) and after being heated (C,D). After being heated, the NCs showed segregation presenting a core-shell structure. Before heating, the NC are on average 151nm. After heating, the NC are reduced slightly in size to 140nm total. Based on the aqueous environment, it is hypothesized that the outer shell is composed of mostly silica and the core contains P4VP considering its hydrophobicity. By weight, the NC are 66% TEOS and 34% P4VP while the cores are around 92nm and the shells are 23nm. If the hypothesis is true, then the silica appears to have condensed in volume which is likely due to containing the P4VP in the cores. Since there is less P4VP in the NCs, the cores seem slightly swollen which could be due to ethanol getting trapped in the center which allows for the stabilization of the P4VP in the aqueous environment.

The age of the NCs and storing solvent play an important role in whether or not the NCs will segregate upon heating. If the NCs were freshly made, then they would not segregate upon heating. The NCs must also be stored in ethanol for an extended period of time. The segregation worked for NCs that had been stored in ethanol for both 4months and 1year. The minimum amount of time needed to age in order for the NCs to segregate still needs to be studied. NCs that were stored in water for 1year were also tested, however the NCs showed no signs of segregation. Since water hydrolyzes TEOS in order to form silica when the NCs are stored in water for extended periods of time, the silica becomes more rigid and less mobile due to cross-linking. The benfit of using ethanol is the TEOS does not cross-link which allows for some mobility. It also allows for the mobility of the P4VP within the NC.

The NCs composed of P4VP and silica have also been shown to be affected by changes in pH which can be seen in Figure 2.2. The NCs were in an aqueous solution and either 0.5M HCl or 0.5M NaOH was added in order to change the pH to the desired

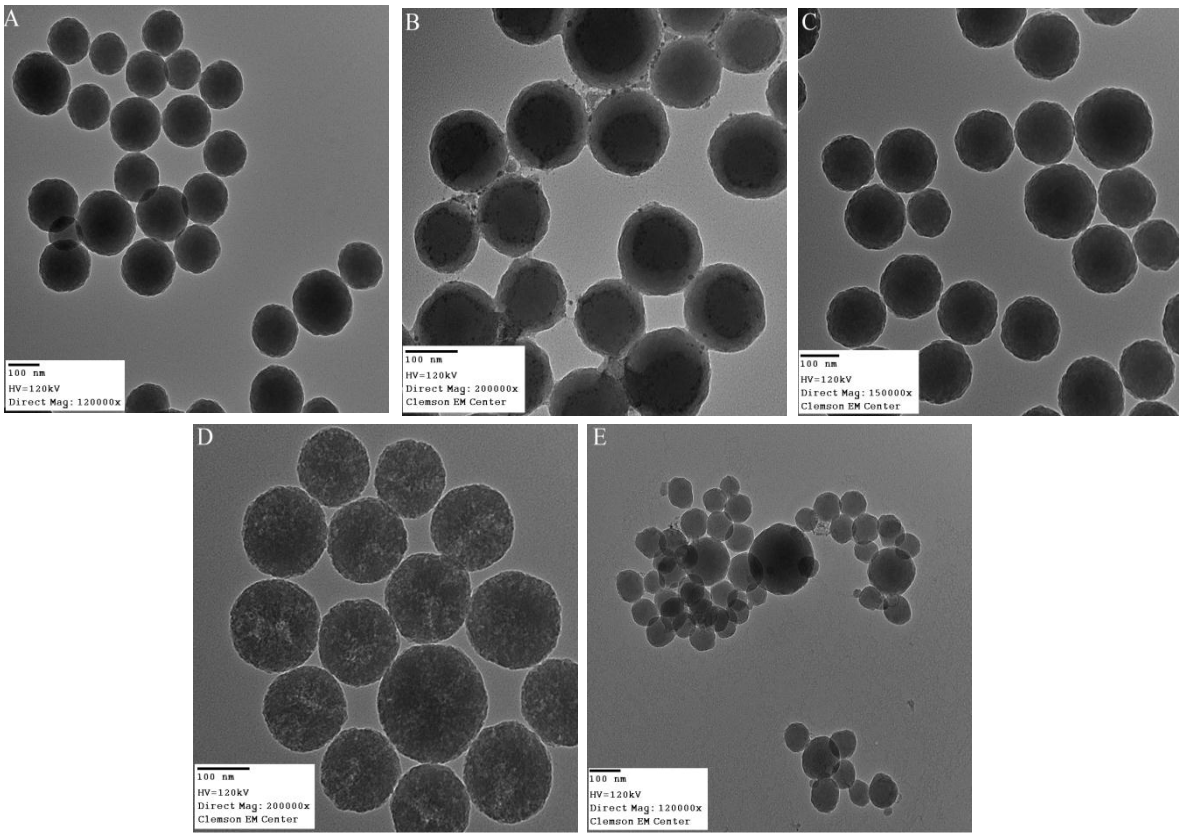

Figure 2.2. TEM images of nanocomposites as a result of changes in pH. Nanocomposites at pH 7 (A), pH 3 (B), pH 5 (C), pH 9 (D), and pH 11 (E)

value. Figure 2.2A shows the NC in water with a pH of 7. It is noted that the NCs are polydisperse with a range of 60nm to 150nm which is not favorable due to varying particles sizes having different interactions with light. Even though the NCs are polydisperse, they were still used for the pH studies. Figure 2.2B shows the NC in a pH 3 solution where there is a clear segregation inside the NC. It is hypothesized that the outer

shell is composed of P4VP and the core is silica based on the pKa values and stability of the materials. The pKa of silica is about 4 so it is insoluble in extreme acidic conditions due to the postitive charge after protonation. P4VP is typically insoluble in water and will form particles in normal aqueous environments. However, when P4VP is added to an acidic aqueous environment in the pH range of 3-6 it becomes soluble. The pKa of pyridinium is 5.25, so in lower acidic solutions it is protonated giving it a positive charge and allowing it to be miscible in water. Since the NC is still suspended in the aqueous solution, based on our hypothesis, the pyridine is keeping the silica from precipitating out of solution. The segregation shown in figure 2.2B appears to be the opposite of the segregation shown in figure 2.2D which supports the claim that the shells are composed of two different materials. Figure 2.2C shows the NC in a pH 5 solution where the speration of the P4VP and silica is less clear. From the figure, it appears the NC may be starting to separate, but it is not pertinent for a complete segregation to occur to keep the NC soluble at that pH. At a pH of 5, the silica has a negative charge on the surface making it stable in water, while P4VP is still mostly protonated and thus also stable. Figure 2.2D shows the NC in a pH 9 solution. There does not appear to be any sort of clear separation in the particles, but the particles have a roughness to them and there was some precipitate on the bottom of the vial. This suggests that the silica is being etched away by the basic conditions and the P4VP is being exposed causing it to precipitate out due to its deprotonated state. Figure 2.2E shows the NC in a pH 11 solution which had to be sonicated back into solution since it had precipitated out. This figure further supports the conclusion that the silica has been etched away since the majority of the particles are

about half the size of the starting NCs. The resulting particles consist of mostly P4VP which are insoluble in the basic aqueous environment.

Although the NCs have shown to segregate under various conditions, there are still many experiments that need to be conducted and reproducibility needs to be looked at further. If segragation can occur using silica/P4VP, then other polymers may behave in the same manner and polymers with different polarities can be examined. Since both silica and P4VP behave similiarly in most solvents, the segregation of the NCs while heating has only in one formation with the silica as the outer shell. In order to get the NCs to segregate with the silica as the core and polymer has the shell would be to use a different polymer. One polymer to try is polystyrene which was synthesized in the originial paper by Sertchook and Avnir[15]. PS is insoluble in polar solvents, so by heating NCs composed of silica/PS in toluene and heated in water should give a similar segragation with silica as the shell. However, if the NCs are dispersed in water and then heated in toluene, the NCs may segregate with the PS as the shell. NCs have many potential applications with both segregated and unsegregated conformations and will need to be further explored.

CHAPTER THREE

SYNTHESIS OF VARIOUS COPPER PARTICLES IN THE PRESENCE OF POLY(ACRYLIC ACID)

Introduction

Both silver and copper have been found to have antimicrobial properties which are of great interest due to their use as disinfectants in health care as well as in wastewater treatments.[16,17] However they are both considered cytotoxic which limits their use, especially in biological systems, unless they are modified. This chapter will focus on a new method of synthesizing stable copper oxide nanoparticles which involves the formation of a tetraammineaquacopper (II) complex[38] with poly(acrylic acid) (PAA) as a stabilizer. In addition to the copper oxide nanoparticles, copper (I) iodide and copper (II) sulfide particles with PAA were also synthesized. The goal of this project is to develop various copper particles and test their antimicrobial properties in biological systems.

Experimental Methods

Materials: Copper (I) oxide (Cu_2O) and sodium sulfide (Na_2S) were purchased from Sigma Aldrich. Anhydrous cupric sulfate (Cu_2SO_4) was purchased from Mallinckrodt. Potassium iodide (KI) and 5000 MW Polyacrylic acid (PAA) were received from Acros. Sodium borohydride ($NaBH_4$) and 29.3% ammonium hydroxide were purchased from Fisher Scientific. High purity nitrogen gas was received from AirGas.

Copper Oxide Nanoparticle Synthesis: A stock solution of 120ppm copper solution is made by first dissolving 12mg Cu_2O completely in 10mL NH_4OH before diluting with 90mL of ultrapure 18MΩ H_2O. In a 20mL scintillation vial, 10mL of the 120ppm copper stock solution and 50µL of a 1% (w/w) PAA were added. In a separate 1dr vial, 2mg $NaBH_4$ was dissolved in 2.5mL H_2O and sonicated briefly to mix before injecting 2mL of the $NaBH_4$ solution directly into the copper solution. The vial was capped and swirled until it turned a uniform light yellow or yellow-brown. It was allowed to age for 1hour until it turns a deep red color. The solution was then bubbled with N_2 gas until all of the NH_4OH has been removed. The vial was capped quickly to prevent the least amount of air from entering the vial.

Copper Iodide Particle Synthesis: In an Erlenmeyer flask, 78.8mL of 0.2M copper (copper (II) sulfate) and 7.8mL of 20% (w/w) PAA was mixed. Then 100mL of 0.4M iodide (potassium iodide) was added to the flask and thoroughly mixed producing a white powder. An additional 50mL of 0.4M iodide solution was added to complete the reaction. The powder was washed with water by centrifugation four times before drying in a vacuum oven at 50°C.

Copper Sulfide Particle Synthesis: In an Erlenmeyer flask, 78.8mL of 0.2M copper (copper (II) sulfate) and 7.8mL of 20% (w/w) PAA was mixed. Then 100mL of 0.2M sulfide (sodium sulfide) was added to the flask and thoroughly mixed producing a dark powder. An additional 50mL of 0.2M sulfide solution was added to complete the reaction. The dark bluish-black powder was washed with water by centrifugation four times before drying in a vacuum oven at 60°C.

Microscopy Characterization: The samples were dried on a formvar coated copper grid purchased from Ted Pella and imaged using the TEM-Hitachi H7600T.

Results and Discussion

In the beginning metallic copper nanoparticles was desired, however it is difficult to stabilize the copper in metallic form. Instead, copper oxide nanoparticles were synthesized since it was easier to stabilize them over longer periods of time. Most methods for growing copper nanoparticles with poly(acrylic acid) (PAA) as a stabilizing agent uses soluble copper salts, such as copper (II) sulfate[39,40,41] and copper (II) acetate,[42] however we developed a method that uses copper (I) oxide in ammonium hydroxide which forms a tetraammineaquacopper (II) complex. Copper (I) oxide (Cu_2O) has a very low solubility in water, however by adjusting the pH it will become soluble[43] which is where the ammonium hydroxide (NH_4OH) plays a role. First, Cu_2O, a red powder, was dissolved in NH_4OH producing the tetraammineaquacopper (II) complex. Low molecular weight PAA was added to the copper solution so that the concentration of PAA is 0.005%. The copper ions were then reduced using an excess of sodium borohydride generating a deep reddish color upon aging signifying copper metal nanoparticles. The nanoparticles were allowed to age for approximately one hour before the NH_4OH was removed by bubbling with N_2. If the NH_4OH was not removed from the copper nanoparticles, the copper would precipitate out into a black powder resembling CuO. As the copper metal nanoparticles are allowed to sit, they begin to turn a dark green color which will fade to a pale green over time. The change in solution color from red to green

is the result from the metallic copper oxidizing.[40] The final nanoparticle size are very small with an average diameter of about 4.5nm (figure 3.1).

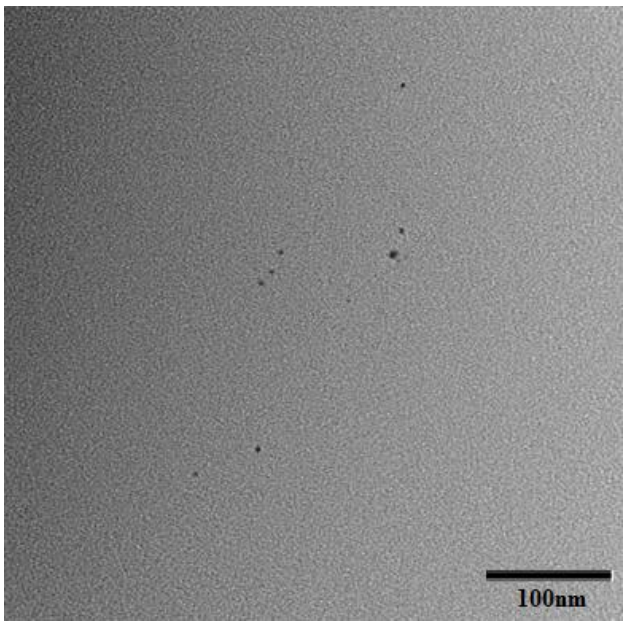

Figure 3.1. TEM image of copper oxide nanoparticles.

The form of copper oxide in the nanoparticle, whether it is CuO or Cu_2O is not yet known and must be further explored. A question that remains from the reaction with copper (I) oxide, is what part does the ammonia play in the reaction? In the beginning of the reaction, the copper and ammonia form a tetraammineaquacopper (II) complex which results in a deep blue color. When the sodium borohydride is added, the copper is reduced to copper metal and changes from blue to red. What happens to the copper-ammonia complex needs to be further explored to determine if the ammonia is still present and integrated into the copper nanoparticle or if it is all removed during the reduction process and bubbling with N_2. The ammonia obviously plays an important role

if you look at the progression of the reaction. In the beginning it is used simply to dissolve the copper (I) oxide, but if it is not removed, then the copper will end up precipitating out. One suggestion as to the precipitation is that the PAA and the NH_4OH are reacting through acid/base chemistry causing the PAA to no longer be able to stabilize the copper after prolonged exposure to the base. The copper then oxidizes and precipitates out as CuO before dissolving in the ammonia solution once again. The tetrammineaquacopper (II) complex with PAA present reacted unexpectedly with acetone which was another reason the role of ammonia was considered important. In the literature, when acetone is added to PAA which have absorbed copper ions, it will precipitate out.[44] Upon the addition of metallic copper nanoparticles, before the removal of NH_4OH, to an excess of acetone, the solution turned almost completely clear but with a slight blue tint with no precipitate forming at any point. So, the ammonia present seems to be preventing the PAA from precipitating out yet the copper-ammonia complex is reforming almost immediately. However, once the ammonia is removed and the metallic copper oxidizes, the addition of acetone does not result in a color change and overtime will precipitate out. If the copper oxide nanoparticles are allowed to set undisturbed the color will continually fade, but they will not precipitate out.

In addition to the copper oxide nanoparticles, copper (II) sulfide and copper (I) iodide (CuI) particles were synthesized. Both the CuS and CuI particles need to be characterized by electron microscopy in order to determine the size and whether they can be classified as a nanoparticle. Due to the precipitation of the particles, it is likely to

assume they are in the micrometer size range. The chemical reactions for both particles are shown below:

$$CuSO_4 + 2KI \rightarrow CuI + K_2SO_4 + \tfrac{1}{2} I_2 \quad (3)$$

$$CuSO_4 + Na_2S \rightarrow CuS + Na_2SO_4 \quad (4)$$

Both the iodide and sulfide copper particles were synthesized starting with $CuSO_4$ and PAA, which is not shown in the above reactions. For CuI particles, PAA was added to the $CuSO_4$ solution so that the concentration of polymer was 1.8% by weight. An excess of KI was added which created a white precipitate and yellow supernant indicating the formation of iodine which is a byproduct from the reaction. The CuS particles were synthesized in the same manner as the CuI particles with the Na_2S replacing the KI. An excess of Na_2S was added to the $CuSO_4$ which resulted in a bluish-black precipitate with a clear green supernant.

The copper oxide nanoparticles have shown success in their use against bacterial cells, however the concentrations of nanoparticles needed to kill the bacteria is too high for mammalian cells. The three different particles synthesized are also currently being explored for their use in dental implants as an antimicrobial agent.

CHAPTER FOUR

SERS ACTIVE SILVER COATED ALUMINA MEMBRANES

Introduction

As discussed in chapter 1, previous work has been done using silver deposited on different types of alumina as SERS substrates. Porous alumina membranes have been used as SERS substrates by depositing silver either chemically, by vapor deposition, or filtering colloids. The benefits of using a porous membrane design is the ability to filter dilute organic solutions through the pores in order to concentrate the sample and enhance Raman signals. This chapter focuses on the use of silver chemically deposited on porous alumina membranes by a simple ethanol reduction of Ag_2O. Dilute adenine solutions were filtered the through the coated alumina membranes producing a strong Raman signal.

Experimental Methods

Materials: Silver (I) oxide (99.99%) was purchased from Alfa Aesar and adenine was purchased from Sigma Aldrich. Absolute 200 proof ethanol was purchased from Pharmco-AAPER. High purity nitrogen gas was received from AirGas. The alumina membranes (Anodisc 13 and 32) were purchased from Whatman with pores either 0.1μm or 0.2μm in diameter and the glass slides were purchased from VWR.

Glass Slide Procedure: The glass slides were first put through a cleaning process of being washed with soapy water, rinsed with 18MΩ water, dried with a N_2 air stream and plasma cleaned (Harrick Plasma Cleaner/Sterilizer PDC-32G) for about 1min. After cleaning, the slides were added to approximately 25mg of Ag_2O and 5mL of absolute

ethanol that had been sonicated in a 1dr vial to disperse the Ag_2O. The slides were allowed to roll for 3-8hours, unless otherwise noted, in order to form a thin layer of silver on the surface. The slides were then rinsed and placed in a vial of fresh 18MΩ water in order to run Raman scattering experiments. The glass slides were added to dilute adenine solutions (10-100nM) and allowed to roll for an average of 20min before rinsing and storing with 18MΩ water. Raman scattering experiments were repeated.

Alumina Membrane Procedure: The membranes were first plasma cleaned to obtain a clean surface prior to use. In a typical procedure, approximately 25mg of silver (I) oxide (Ag_2O) and 5mL of absolute ethanol was sonicated in a 1dr vial until the Ag_2O was well-dispersed in the ethanol before adding the alumina membrane. The vial was allowed to roll overnight, unless otherwise noted, in order to form a thick layer of silver on the surface of the substrate. The membrane was then rinsed and placed in a vial of fresh 18MΩ water in order to remove any ethanol left in the pores. A dilute adenine solution (10-100nM) was filtered through the membrane, which was then rinsed three times with fresh 18MΩ water to remove any unattached adenine. When using N_2 gas to remove CO_2 from the surface of the membrane, the ethanol was first bubbled with N_2 for 30minutes before adding the Ag_2O and sonicating briefly. Then the alumina membrane was added and the solution was bubbled for another 30minutes before allowing it to roll overnight.

Raman Experiments: An Argon laser (Innova 200, Coherent) operating at 514.5nm and 18mW at the sample was employed for excitation of Raman scattering. The scattered light was collected by an f/1.2 camera lens in a 1808 backscattering geometry

and analyzed by a triple spectrometer (Triplemate 1877, Spex) equipped with a charge-coupled device (CCD) detector (iDUS 420 series, Andor) cooled to -60°C. Typical spectra acquisition time was 25s. The Raman spectrum of indine was used for spectral calibration.

UV-Vis and Microscopy Characterization: A Schimadzu UV-2501PC was used to colled UV-Vis spectra and Hitachi FE-SEM SU6600 was used to image the alumina membranes.

Results and Discussion

A simple reduction of Ag_2O by ethanol[45] was used to produce silver films on different substrates. Since Ag_2O has a low solubility in ethanol, the exact concentration in solution was not determined instead the mass of Ag_2O added was monitored. While the concentration did not appear to have a large effect on the thickness of the silver layer on alumina or glass slides, the amount of Ag_2O did need to be adjusted based on the size of the substrate/reaction vessel. Since the vessel will also be coated with silver, larger substrates require slightly more Ag_2O due to the larger surface area needing to be coated.

Preliminary experiments were conducted on glass slides before using the alumina membranes. Since Ag_2O has a low solubility in ethanol, there are fewer ions in the solution to be reduced which results in only small amounts of Ag NPs in the solution and most of the silver is reduced onto the surface of both the vial and substrates. Due to the low solubility, the substrate should remain in contact with the Ag_2O in order to increase the probability of obtaining a silver film. Experiments were conducted where vials containing Ag_2O and ethanol were allowed to either roll or sit stationary overnight to test

the contact effect of Ag_2O and the substrate. The vial that was allowed to sit overnight had a thick mirrored film on the bottom of the vial while the sides were a slight brown indicating a thin layer of silver. In comparison, the entire surface of the vial that was allowed to roll overnight had a mirrored film indicating a thick silver layer. The same experiment was repeated, but with the addition of glass slides in the reaction vessels in order to monitor the change by UV-Vis. Both slides came in contact with the Ag_2O initially; however the rolling reaction came in constant contact with all the Ag_2O. By rolling the reaction, there were fewer limitations on how much silver could be deposited on the slide. The rolling light reactions produced a thicker film indicated by the UV-Vis curve in figure 4.1 where the peak is shown to have the highest absorbance at a higher wavelength. The stationary light reaction peak has a lower absorbance at a lower wavelength indicating a thinner film.

The presence of light was also shown to play a role in the formation of silver films. Experiments were setup with glass slides placed in ethanolic Ag_2O solutions and allowed to react by rolling and sitting in ambient light overnight as well as placed in the dark overnight. As discussed in the previous paragraph, each of the glass slides had some contact with Ag_2O during the entire process. The rolling reaction was constantly in contact with all the Ag_2O while only a small amount of Ag_2O stuck to the other stationary (light and dark) samples. Each of the slides had a thin yellow film of silver which suggests that light is not a requirement for this reaction. Even though light is not required for the reduction process, it does help in increasing the reaction rate as can be seen by the UV-Vis data in figure 4.1. The reactions that were exposed to ambient light, whether

rolling or stationary, produced slides that had thicker films than the reactions that were kept in the dark.

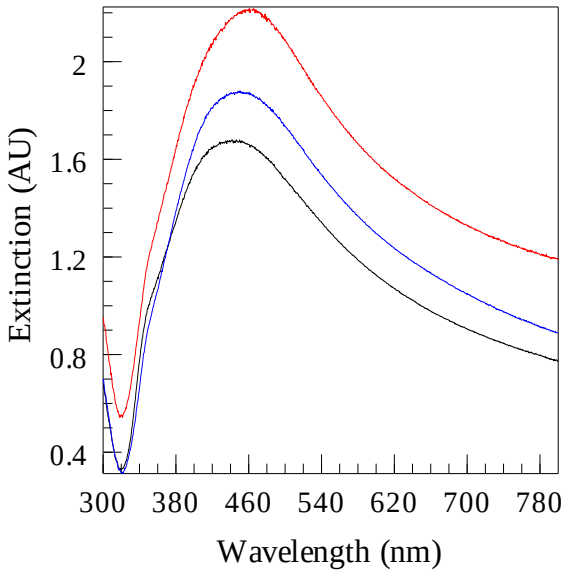

Figure 4.1. UV-Vis spectral series of silver reduced onto glass slides via the chemical reduction of silver (I) oxide by ethanol where the reaction was took place in the dark (black), stationary in ambient light (blue) and rolling in ambient light (red).

The biggest factor in determining film thickness is the reaction time so that as the exposure time increases so does the film thickness (figure 4.2). After about two hours, the silver films appear as a light brown with the maximum wavelength at 411nm which suggest that the film is composed of small Ag NPs. As time progresses the Ag NPs on the surface of the substrate become larger and more dense causing the maximum wavelength to red-shift and the absorbance to increase (figure 4.2).

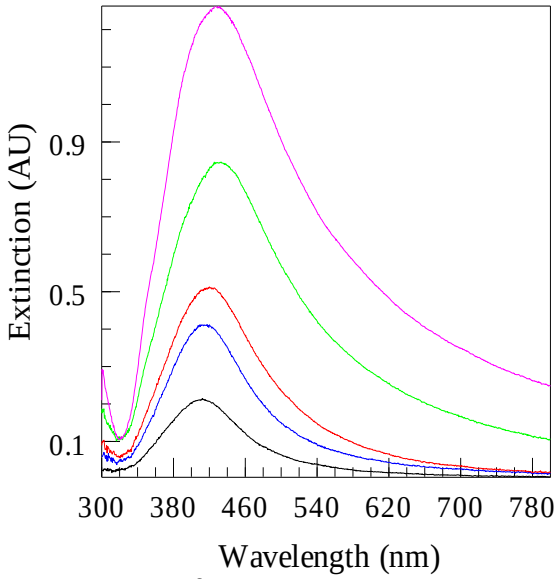

Figure 4.2. UV-Vis spectral series of silver reduced onto glass slides via the chemical reduction of silver (I) oxide by ethanol where the reaction was allowed to roll for 3hr (black), 4hr (blue), 5hr (red), 6hr (green), and 7hr (pink).

After preliminary data on glass sides, alumina membranes were used. Alumina membranes went through a slightly different color change than the glass slides. After about 2 hours the membranes appeared yellow and after about 18 hours they were a deep reddish-black. If allowed to sit in the Ag_2O and ethanol reaction vessel the membrane will begin to appear reddish-black and with extended reaction times will turn a dull gray. Since Ag_2O contact with glass slides appeared to be important, the alumina membrane reactions were allowed to roll each time. Similar results were found with the alumina membranes when comparing reactions that were in ambient light and in darkness where the light increased the reaction rate. Like the glass slides, the effect of reaction time was the most important factor in determining film thickness. Figure 4.3 shows the UV-Vis results of reaction time on the alumina membrane. Uncoated alumina does not produce a

single peak, but instead it slowly increases in intensity before leveling off. As the reaction proceeds, the curves begin to steepen and level off at higher wavelengths.

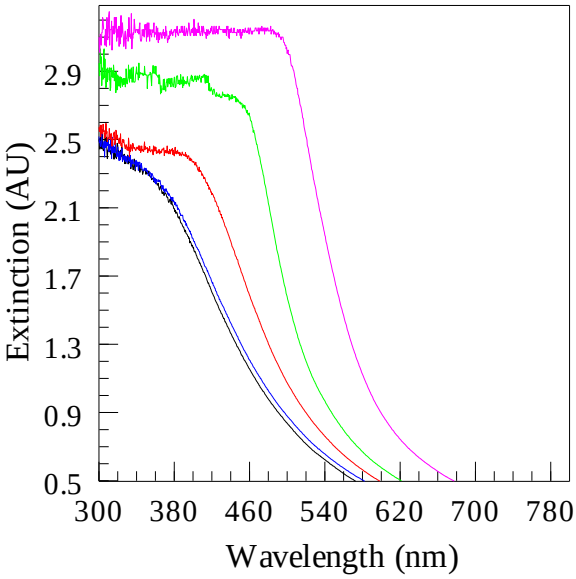

Figure 4.3. UV-Vis spectral series of silver reduced onto alumina membranes with a pore diameter of 200nm via the chemical reduction of silver (I) oxide by ethanol where the reaction was allowed to roll for 3hr (black), 4hr (blue), 6hr (red), 8hr (green), and 23hr (pink).

Figure 4.4 shows the deposition of various thicknesses of silver films on alumina membranes. Figure 4.4A shows the SEM image of a plain alumina membrane that was carbon coated in order to get an image. The surface of the plain alumina appears to be coated with a thick layer of carbon that forms long chains and settles on top of the alumina membranes. As the silver thickness increases, long chains are formed on the surface, similar to what is seen with the carbon coating which is shown in figures 4.4B and 4.4C. Silver is depositing onto the surface of the alumina which is apparent in the color changes of the alumina however the long chains could be due to graphitization

occurring on the surface of the membrane and will be discussed later in this chapter. The resolution on the instrument did not allow for the clear zoomed-in images needed to determine where or how the silver is depositing, whether it is depositing inside the pores and what it looks like on the surface. In figure 4.4B, the majority of the 100nm pores

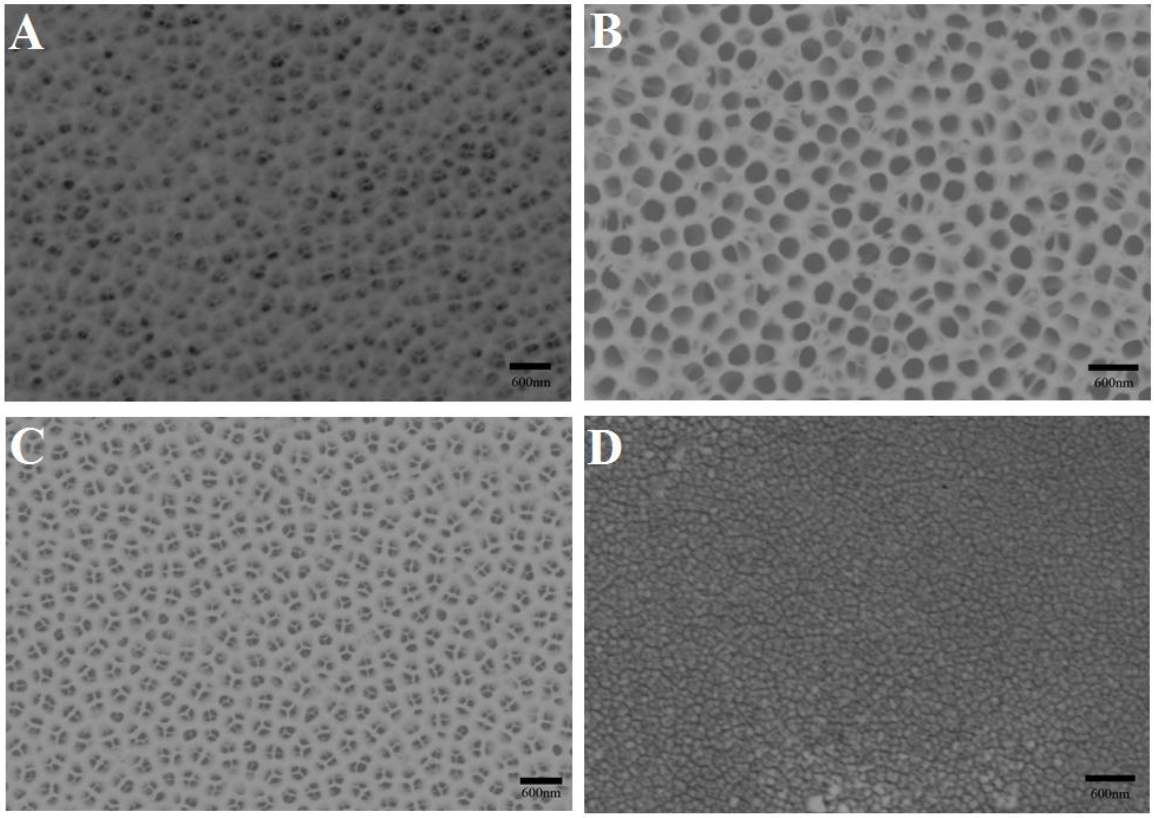

Figure 4.4. TEM images of carbon coated alumina membrane (A), a thin layer of silver (B), a medium layer of silver (C), and a thick layer of silver (D).

appear to still be open with some pores completely covered by a thin layer of silver which causes the alumina membrane to visually appear a light yellow. In figure 4.4C, most of the 100nm pores were covered by the silver creating a thicker layer on the surface which gives the membrane a reddish-black color. There were also aggregates of silver

nanoparticles on the surface of the membrane as thicker layers are grown. The thin silver layers had very few to no silver nanoparticles on the surface. Figure 4.4D shows an alumina membrane that appeared black, but when looking through it was a deep red. The silver layer in figure 4.4D is very thick and covers the majority of the pores which gives it a rough morphology. As the thickness of the silver layer increases on the alumina membrane, it does become slightly more difficult to filter the adenine solutions through since the pores become covered. Sample 4.4D will be slightly harder to filter a solution through as opposed to sample 4.4B. The optimum time for the silver deposition was determined to be around 14-18hours to allow for a thick coating, but still able to easily filter a solution through the membrane. This time allotment also produced the least amount of background in the Raman studies.

Adenine was used in the Raman scattering experiments since it readily absorbs to silver and gives a strong Raman signal at 738cm^{-1}. It was noticed that the thickness of the silver layer affected the background Raman spectra greatly when using the Ag_2O and ethanol reduction method. If the silver layer was too thin presenting a predominantly yellow color, then the sample would fluoresce and an adenine peak could not be obtained. If the silver layer was too thick presenting a black or gray color, then the membrane would give strong sharp Raman peaks which made it difficult to observe weaker adenine signals. In figure 4.5, the black line is the Raman scattering from a 1min plasma cleaned alumina membrane with no silver deposited. The baseline is mostly flat with a small broad peak at about 1650cm^{-1} which will rule out the fluorescence or sharp Raman peaks as the direct results of the alumina membrane.

In order to determine the cause of the fluorescence and Raman peaks, different depositions methods of silver were tested and compared to the chemical deposition of Ag_2O and ethanol. First, a dilute 100nm silver nanoparticle (Ag NP) solution was filtered through the alumina membrane. Most of the Ag NPs deposited onto the surface of the membrane giving a light yellow to dull gray color depending on the concentration and

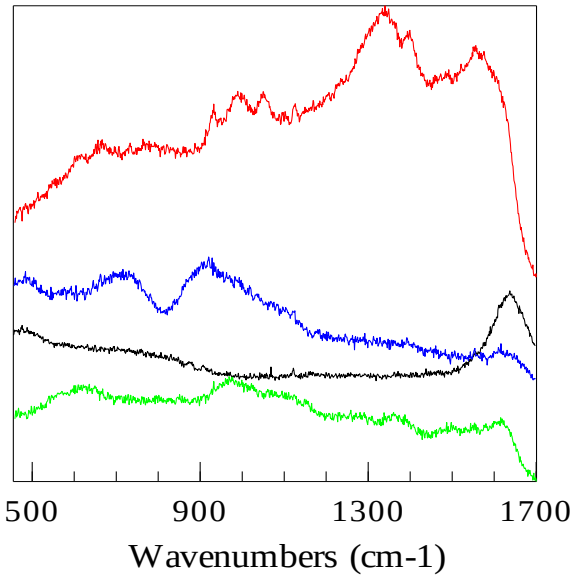

Figure 4.5. Raman spectra of alumina membranes with a pore diameter of 100nm (black) with Ag NPs on the surface (blue) and 30nm vapor deposited film without plasma treatment (red) and with plasma treatment (green).

amount of particles filtered. The blue line in figure 4.5 depicts the Raman scattering from the filtered Ag NPs on the membrane, where there are no sharp peaks and a relatively flat background. It should be noted that there are no peaks at the higher wavenumbers. The next method tried was vapor depositing 30nm of silver onto the surface of alumina membranes to create a thin film. The silver was deposited on alumina

that was either plasma treated for 10min (green line) or had no plasma treatment (red line) as seen in figure 4.5. There was a significant difference in the spectra when comparing the plasma treated sample vs. the membrane with no plasma treatment. Without plasma treatment, there is more Raman scattering at the higher wavenumbers as well as a stronger background which would mask small adenine signals. When the

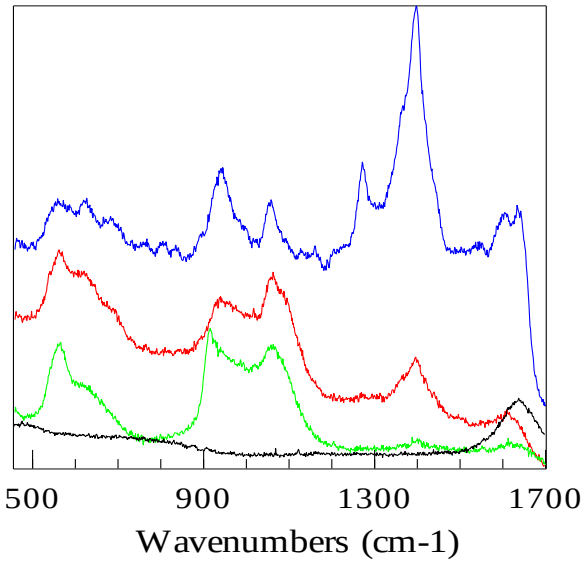

Figure 4.6. Raman spectra of silver reduced onto alumina membranes with a pore diameter of 100nm (black) via the chemical reduction of silver (I) oxide by ethanol and bubbling N2 gas. The alumina membranes were plasma cleaned for 1min (blue), 5min (red), and 10min (green) prior to deposition.

sample was plasma treated for 10min or more, the scattering from the silver decreased and the background became more flat.

When observing the spectra from the silver deposited on the non-plasma treated alumina, it was noted that it resembled Raman spectra obtained from graphite.[46] The peaks at the higher wavenumbers are believed to have been caused by graphite depositing

on the surface of the spectra due to absorbed CO_2 on the membrane during the reduction process. To test this theory, CO_2 would need to be removed from the reaction which was done by bubbling the solution with N_2. In addition, different plasma treatment times were also measured to test the effect it played on the reaction. The ethanol was bubbled with N_2 gas for 30min before the Ag_2O and plasma treated alumina (1min, 5min, and 10min treatment times) were added and allowed to bubble for another 30min with the N_2 before rolling overnight. The results are shown in figure 3.6. Using a mixture of bubbling N_2 and long plasma treatment times, the sharp peaks and background at higher frequencies are eradicated. There are still some broad peaks at the lower wavenumbers, but they did not interfere directly with the adenine peak at 738cm^{-1}. Another way to

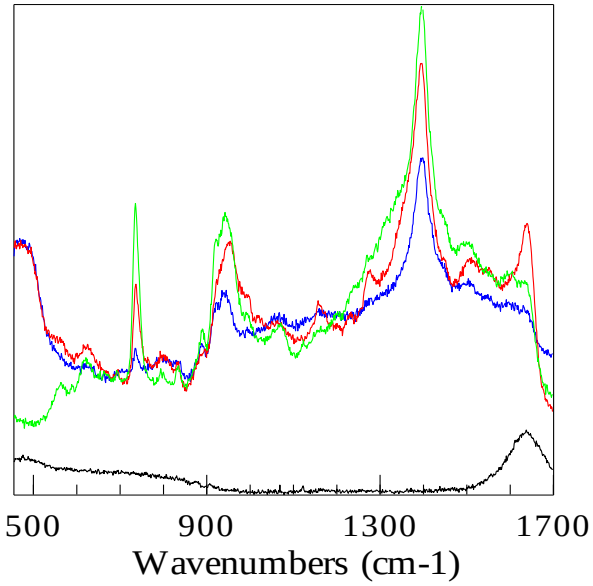

Figure 4.7. Raman spectra of adenine on silver reduced onto alumina membranes with a pore diameter of 200nm (black) via the chemical reduction of silver (I) oxide by ethanol with adenine concentrations of 10nM (blue), 50nM (red), and 100nM (green).

decrease the formation of graphite is to use a longer wavelength for excitation. Bello et. al.[30] reported a decrease in graphite formation by using a 647.1nm excitation wavelength as opposed to 514.5nm.

The chemical deposition of silver on alumina produced a sensitive method for detecting adenine. Silver coated by vapor deposition alumina membranes have been used previously to detect dilute solutions of molecules, and seemed to have similar results to what has been produced here. Figure 4.7 shows the Raman scattering spectra produced from different concentrations of adenine adsorbed onto the silver surface of the alumina. Concentrations as low as 10nM of adenine were still able to be detected by showing the peak at 738cm^{-1}. From the spectra, there is a higher background at the higher wavenumbers which is likely due to graphite forming on the membrane.

Most SERS substrates which typically require more concentrated molecule solutions than nanomolar to adsorb onto the surface in order to get any Raman signal. More dilute solutions can be used; however the time needed for the substrate to interact with the molecule solution would need to be increased. Porous alumina membranes have the benefit of being able to filter dilute solutions in order to concentrate them and get a stronger signal. This is a quick process and has the potential to be used for biological samples which are typically lower concentrations and small amounts.

CHAPTER 5

CONCLUSION AND FUTURE WORK

This thesis presented the synthesis of different nanoparticles and nanostructures which have the potential to be used in biological systems. Chapter 2 focuses on the synthesis of NCs composed of silica and P4VP in a NH_4OH and ethanol solution. The sizes of the NCs are easily controlled by adjusting the concentrations of reagents used. Increased amounts of NH_4OH produce large NCs while higher concentrations of P4VP results in smaller NCs. Heat and changes in pH have been shown to cause the NCs to segregate internally. When NCs are stored in ethanol for extended periods of time (months-year) and then heated in water a core-shell nanostructure is formed. It is hypothesized that the shell is composed mostly of silica while the core is P4VP due to its hydrophobic nature. The opposite core-shell nanostructure appears to form when the NCs are added to an acidic aqueous solution. At low pHs, P4VP is stable in aqueous environments which allows it to form a shell around the silica that is unstable in acidic conditions. At higher pHs, the NCs appear to decompose and precipitate out due to the silica being etched away and exposing P4VP. Future work on NCs will include synthesizing with polymers that exhibit different properties than those of P4VP. The goal is to get the NCs to segregate one way when heated in one solvent and the opposite when heated in a different solvent with the process being reversible.

In chapter 3, a novel synthesis method of growing stable copper oxide nanoparticles from insoluble copper (I) oxide and PAA is presented. Since copper (I) oxide is insoluble initially it is dissolved in ammonium hydroxide before diluting with

water. The copper and ammonium hydroxide forms a tetraammineaquacopper (II) complex which plays a vital role in the reaction and needs to be further explored. The form of copper oxide, CuO or Cu_2O still needs to be determined. The nanoparticles are around 4.5nm which makes their size perfect for the use with cells. Copper (I) iodide and copper (II) sulfide particles were synthesized as well, but still need to be characterized by electron microscopy in order to determine their sizes. All of the copper particles will be tested for their use as antimicrobial agents in dental implants.

Chapter 4 discusses the use of silver coated alumina membranes as SERS substrates. Alumina membranes with pores either 100nm or 200nm in diameter were coated with silver by reducing Ag_2O with ethanol. Concentration of Ag_2O was not an important factor in determining the thickness of the silver layer on the membranes. The membranes exposure time to the Ag_2O and ethanol determined the thickness of the silver film. It was determined that between 14-18hrs exposure time produced the desired thickness of silver. If the membrane was in contact for more than 24hrs, the background produced strong Raman signals and it became too difficult to filter the adenine solution through. If the membrane was exposed for 10hrs or less, the membrane would fluoresce under laser irradiation and no signal could be determined. Dilute (10-100nM) adenine solutions were filtered through the membranes in order to concentrate the samples on the surface. Even though some SERS substrates are able to enhance an adsorbed 10nM solution of adenine, the time the substrate must be exposed to the solution increases the lower the concentration.

REFERENCES

[1] Salata, O.V. *Journal of Nanobiotechnology.* **2004**, *2:3*

[2] Shipway, A.N.; Katz, E.; Willner, I. *Chem. Phys. Chem.* **2000**, *1*, 18-52

[3] Genger, U.R.; Garbolle, M.; Jaricot, S.C.; Nitschki, R.; Nann, T. *Nat. Methods.* **2008**, *5*, 763-775

[4] Farokhzad, O.C.; Langer, R. *ACS Nano.* **2009**, *3*, 16-20

[5] Petros, R.A.; DeSimone, J.M. *Nat. Rev. Drug. Discov.* **2010**, *9*, 615-627

[6] Zhang, L.; Gu, F.X.; Chan, J.M.; Wang, A.Z.; Langer, R.S.; Farokhzad, O.C. *Clin. Pharmacol. Ther*. **2008**, *83*, 761-769

[7] Douglas, F.; Yanez, R.; Ros, J.; Marín, S.; Muniz, A.E.; Alegret, S.; Merkoçi, A. *J. Nanopart. Res.* **2008**, *10*, 97-106

[8] González, B.R.; Burrows, A.; Watanabe, M.; Kiely, C.J.; Marzán, L.M.L. *J. Mater. Chem.* **2005**, *15*, 1755-1759

[9] Tam, F.; Moran, C.; Halas, N.J. *J. Phys. Chem. B.* **2004**, *108*, 17290-17294

[10] Oldenburg, S.J.; Averitt, R.D.; Westcott, S.L.; Halas, N.J. *Chem. Phys. Letters.* **1998**, *288*, 243-247

[11] Chen, Z.; Wang, Z.L.; Zhan, P.; Zhang, J.H.; Zhang, W.Y.; Wang, H.T.; Ming, N.B. *Langmuir*. **2004,** *20*, 3042-3046

[12] Zhang, K.; Chen, H.; Chen, X.; Chen, Z.; Cui, Z.; Yang, B. *Macromol. Mater. Eng.* **2003**, *288*, 380-385

[13] Soppimath, K.S; Liu, L.H.; Seow, W.Y.; Liu, S.Q.; Powell, R.; Chan, P.; Yang, Y.Y. *Adv. Funct. Mater.* **2007**, *17*, 355-362

[14] Singh, N.; Karambelkar, A.; Gu, L.; Lin, K.; Miller, J.S.; Chem, C.S.; Sailor, M.J.; Bhatia, S.N. *J. Am. Chem. Soc.* **2011**, *133*, 19582-19585

[15] Sertchook, H.; Avnir, D. *Chem. Mater.* **2003**, *15*, 1690-1694

[16] Ruparelia, J.P.; Chatterjee, A.K.; Duttagupta, S.P.; Mukherji, S. *Acta Biomaterialia*. **2008**, 4, 707-716

[17] Ren, G.; Hu, D.; Cheng, E.W.C.; Vargas-Reus, M.A.; Reip, P.; Allaker, R.P. *International Journal of Antimicrobial Agent*. **2009**, *33*, 587-590

[18] Ostaeva, G.Y.; Selishcheva, E.D.; Pautov, V.D.; Papisov, I.M. *Poly. Sci.* **2008**, *50*, 147-149

[19] Wang, Y.; Biradar, A.V.; Wang, G.; Sharma, K.K.; Duncan, C.T.; Rangan, S.; Asefa, T. *Chem. Eur. J.* **2010**, *16*, 10735-10743

[20] Prucek, R.; Kvítek, L.; Panacek, A.; Vancurova, L.; Soukupova, J.; Jancik, D.; Zboril, R. *J. Mater. Chem.* **2009**, *19*, 8463-8469

[21] Gotoh, Y.; Igarashi, R.; Ohkoshi, Y.; Nagura, M.; Akamatsu, K.; Deki, S. *J. Mater. Chem.* **2010**, *10*, 2548-2552

[22] Fleischmann, M.; Hendra, P.J.; McQuillan, A.J. *Chem. Phys. Lett.* **1974**, *26*, 163-166

[23] Jeanmarie, D.J.; Van Duyne, R.P. *J. Electroanal. Chem.* **1977**, *84*, 1-20

[24] Ru, E.C.L.; Blackie, E.; Meyer, M.; Etchegoin, P.G. *J. Phys. Chem. C.* **2007**, *111*, 13794-13803

[25] Campion, A.; Kambhampati, P. *Chem. Soc. Rev.* **1998**, *27*, 241-250

[26] Xu, H.; Aizpurua, J.; Kall, M; Apell, P. *Phys. Rev. E*. **2000**, *62*, 4318

[27] Vidal, F.J.G.; Pendry, J.B. *Phys. Rev. Lett.* **1996**, *77*, 1163

[28] Jennings, C.; Avoca, R.; Hor, A; Loufyt, R.Y. *Anal. Chem.* **1984**, *56*¸ 2033

[29] Chumanov, G.; Sokolov, K.; Gregory, B.W.; Cotton, T.M. *J. Phys. Chem.* **1995**, *99*, 9466-9471

[30] Bello, J.M.; Stokes, D.L.; Dinh, T.V. *Appl. Spectrosc.* **1989**, *43*, 1325-1330

[31] Li, Y.S.; Wang, Y. *Appl. Spectrosc.* **1992**, *46*, 142-146

[32] Wang, H.H.; Liu, C.Y.; Wu, S.B.; Liu, N.W.; Peng, C.Y.; Chan, T.H.; Hsu, C.F.; Wang, J.K.; Wang, Y.L. *Adv. Mater.* **2006**, *18*, 491-495.

[33] Walsh, R.J.; Chumanov, G. *Appl. Spectrosc.* **2001**, *55*, 1695-1700

[34] Stöber, W.; Fink, A. *J. Colloid Interf. Sci.* **1968**, *26*, 62-69

[35] Ibrahim, I.A.M.; Zikry, A.A.F.; Sharaf, M. *J. Amer. Sci*. **2010**, *6*, 985-989

[36] Rao, K.S.; Hami, K.E.; Kodaki, T.; Matsushige, K.; Makino, K. *J. Coloid. Interf. Sci.* **2005**, *289*, 125-131

[37] Evanoff, D.D.; Chumanov, G. *J. Phys. Chem. B.* **2004**, *108*, 13948-13956

[38] Donnan, F.G.; Thomas, J.S. *J. Chem. Soc., Trans.* **1911**, *99*, 1788-1796

[39] Ostaeva, G.Y.; Selishcheva, E.D.; Pautov, V.D.; Papisov, I.M. *Poly. Sci.* **2008**, *50*, 147-149

[40] Wang, Y.; Biradar, A.V.; Wang, G.; Sharma, K.K.; Duncan, C.T.; Rangan, S.; Asefa, T. *Chem. Eur. J.* **2010**, *16*, 10735-10743

[41] Prucek, R.; Kvítek, L.; Panacek, A.; Vancurova, L.; Soukupova, J.; Jancik, D.; Zboril, R. *J. Mater. Chem.* **2009**, *19*, 8463-8469

[42] Gotoh, Y.; Igarashi, R.; Ohkoshi, Y.; Nagura, M.; Akamatsu, K.; Deki, S. *J. Mater. Chem.* **2010**, *10*, 2548-2552

[43] Palmer, D.A.; Benezeth, P. 14th International Conference on the Properties of Water and Steam in Kyoto, Kyoto, Japan, August 29-September 3, 2004. pp 491-496 (Solubility of Copper Oxides in Water and Steam)

[44] Bakırcıoğlu, Y.; Şeren, G.; Akman, S. *Spectrochimia Acta Part B.* **2000**, *55*, 1129-1133

[45] Liz-Marzán, L.M.; Lado-Tourino, I. *Langmuir* **1996**, *12*, 3585-3589

[46] Reich, S.; Thomsen, C. *Phil. Trans. R. Soc. Lond. A.* **2004**, *362*, 2271-2288